

# REPORT DOCUMENTATION PAGE

Form Approved  
OMB No. 0704-0188

The public reporting burden for this collection of information is estimated to average 1 hour per response, including the time for reviewing instructions, searching existing data sources, gathering and maintaining the data needed, and completing and reviewing the collection of information. Send comments regarding this burden estimate or any other aspect of this collection of information, including suggestions for reducing the burden, to Department of Defense, Washington Headquarters Services, Directorate for Information Operations and Reports (0704-0188), 1215 Jefferson Davis Highway, Suite 1204, Arlington, VA 22202-4302. Respondents should be aware that notwithstanding any other provision of law, no person shall be subject to any penalty for failing to comply with a collection of information if it does not display a currently valid OMB control number. PLEASE DO NOT RETURN YOUR FORM TO THE ABOVE ADDRESS.

1. REPORT DATE 25 April 2017	2. REPORT TYPE Briefing Charts	3. DATES COVERED (From - To) 01 April 2017 - 30 April 2017			
4. TITLE AND SUBTITLE Multi-scale and multi-physics simulations using the multi-fluid plasma model			5a. CONTRACT NUMBER	5b. GRANT NUMBER	
			5c. PROGRAM ELEMENT NUMBER	5d. PROJECT NUMBER	
6. AUTHOR(S) Eder Sousa			5e. TASK NUMBER	5f. WORK UNIT NUMBER Q1AM	
7. PERFORMING ORGANIZATION NAME(S) AND ADDRESS(ES) Air Force Research Laboratory (AFMC) AFRL/RQRS 1 Ara Drive Edwards AFB, CA 93524-7013			8. PERFORMING ORGANIZATION REPORT NUMBER		
9. SPONSORING/MONITORING AGENCY NAME(S) AND ADDRESS(ES) Air Force Research Laboratory (AFMC) AFRL/RQR 4 Draco Drive Edwards AFB, CA 93524-7160			10. SPONSOR/MONITOR'S ACRONYM(S)  11. SPONSOR/MONITOR'S REPORT NUMBER(S) AFRL-RQ-ED-VG-2017-071		
12. DISTRIBUTION/AVAILABILITY STATEMENT Approved for Public Release; Distribution Unlimited. PA Clearance Number: 17211 Clearance Date: 24 April 2017					
13. SUPPLEMENTARY NOTES For presentation at Dartmouth University for an Invited Lecture Prepared in collaboration with ERC. The U.S. Government is joint author of the work and has the right to use, modify, reproduce, release, perform, display, or disclose the work.					
14. ABSTRACT Viewgraph/Briefing Charts					
15. SUBJECT TERMS N/A					
16. SECURITY CLASSIFICATION OF: a. REPORT Unclassified			17. LIMITATION OF ABSTRACT SAR	18. NUMBER OF PAGES 31	19a. NAME OF RESPONSIBLE PERSON Robert Martin  19b. TELEPHONE NUMBER (Include area code) N/A



# MULTI-SCALE AND MULTI-PHYSICS SIMULATIONS USING THE MULTI-FLUID PLASMA MODEL

Éder M. Sousa

ERC INC., IN-SPACE PROPULSION BRANCH (RQRS)  
AIR FORCE RESEARCH LABORATORY  
EDWARDS AIR FORCE BASE, CA

UMass Dartmouth April 25th, 2017

Distribution A: Approved for public release; distribution unlimited  
Clearance No. 17211





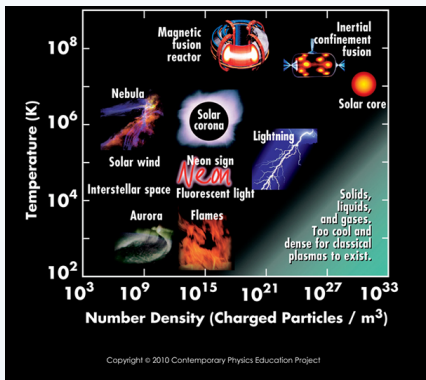
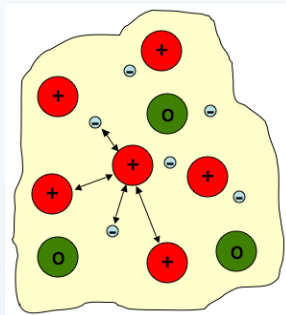
- ① Plasma
- ② Multi-Fluid Plasma Model
  - Advantages
  - Limits of the model
- ③ Numerics: Blended Finite Element Method
  - Discontinuous Galerkin for ion/ neutrals
  - Continuous Galerkin for electrons/ fields
  - Initial tests



# WHAT ARE PLASMAS?



Plasma is a quasineutral gas of charged and neutral particles which exhibits collective behavior.

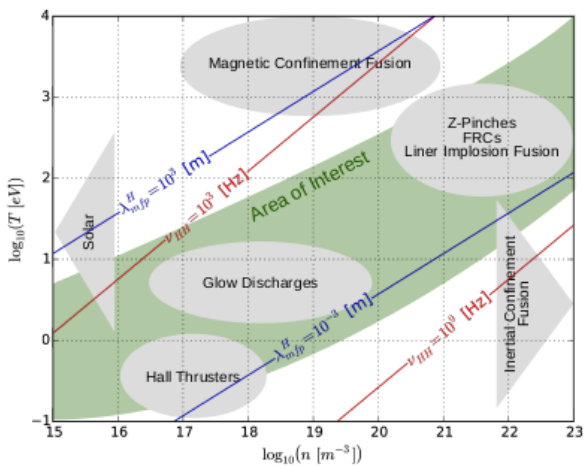


Credit: particleincell.com

- “99% of matter in the universe is in the state of plasma”



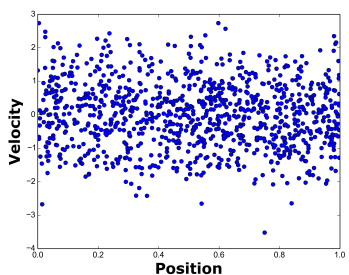
# TIME/SPATIAL SCALES.



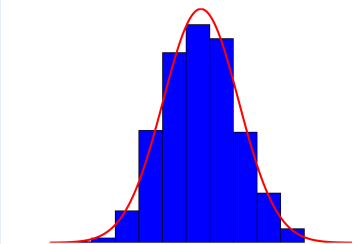
Sean Miller, PhD dissertation, University of Washington (2016)



# THERE ARE MULTIPLE PLASMA MODELS.



- 3-Dimensions + 3-Velocities
- Evolve the particles position and velocity
- e.g. Particle-In-Cell models



- Ensemble average of particles distribution,  $f_s(\mathbf{x}, \mathbf{v}, t)$
- Evolve the distribution function
- e.g. Vlasov-Maxwell models



- The Boltzmann eqn:

$$\frac{\partial f_s}{\partial t} + \mathbf{v} \cdot \frac{\partial f_s}{\partial \mathbf{x}} + \frac{q_s}{m_s} (\mathbf{E} + \mathbf{v} \times \mathbf{B}) \cdot \frac{\partial f_s}{\partial \mathbf{v}} = \frac{\partial f_s}{\partial t} \Big|_c$$

- Take the  $0^{th}$ ,  $1^{st}$ ,  $2^{nd}$  moments of the Boltzmann Eqn.

$$m_s \int \mathbf{v}^n \frac{\partial f_s}{\partial t} d\mathbf{v} + m_s \int \mathbf{v}^{n+1} \cdot \frac{\partial f_s}{\partial \mathbf{x}} d\mathbf{v} + q_s \int \mathbf{v}^n (\mathbf{E} + \mathbf{v} \times \mathbf{B}) \cdot \frac{\partial f_s}{\partial \mathbf{v}} d\mathbf{v} = m_s \int \mathbf{v}^n \frac{\partial f_s}{\partial t} \Big|_c d\mathbf{v}$$

- Each moment of the Boltzmann eqn gives an equation for the moment variable, and introduces the next higher moment variable
- This process can go on indefinitely



$$\frac{\partial \rho_s}{\partial t} + \nabla \cdot (\rho_s \mathbf{u}_s) = \frac{\partial \rho_s}{\partial t} \Big|_{\Gamma}$$

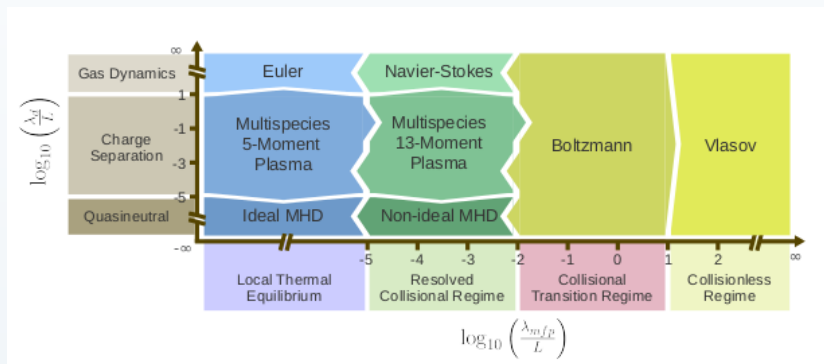
$$\frac{\partial \rho_s \mathbf{u}_s}{\partial t} + \nabla \cdot (\rho_s \mathbf{u}_s \mathbf{u}_s + p_s \mathbf{I} + \Pi_s) = \frac{\rho_s q_s}{m_s} (\mathbf{E} + \mathbf{u}_s \times \mathbf{B}) - \sum_{s*} \mathbf{R}_{s,s*} + \frac{\partial \rho_s \mathbf{u}_s}{\partial t} \Big|_{\Gamma}$$

$$\frac{\partial \varepsilon_s}{\partial t} + \nabla \cdot (((\varepsilon_s + p_s) \mathbf{I} + \Pi_s) \cdot \mathbf{u}_s + \mathbf{h}_s) = \frac{\rho_s q_s}{m_s} \mathbf{u}_s \cdot \mathbf{E} + \sum_{s*} \mathcal{Q}_{s,s*} + \frac{\partial \varepsilon_s}{\partial t} \Big|_{\Gamma}$$

- System is truncated by relating higher moment variables to the lower ones
- The fluids are coupled to each other and to the electromagnetic fields through Maxwell's equations and interaction source terms.



# PLASMA MODELS RANGE OF APPLICABILITY.



Sean Miller, PhD dissertation, University of Washington (2016)



**Kinetic**  $\xrightarrow{\text{LTE, velocity moments}}$  **MFPM**  $\xrightarrow{\epsilon_o \rightarrow 0, m_e \rightarrow 0}$  **MHD**

### IDEAL MHD MODEL IS VALID WHEN:

- High collisionality,  $\tau_{ii}/\tau \ll 1$
- Small Larmor radius,  $r_{Li}/L \ll 1$
- Low Resistivity,  $\left(\frac{m_e}{m_i}\right)^{1/2} \left(\frac{r_{Li}}{L}\right)^2 \frac{\tau}{\tau_{ii}} \ll 1$

### MULTI-FLUID PLASMA MODEL

- Less computationally expensive than kinetic models
- Multi-fluid effects become relevant at small spacial and temporal scales
- Finite electron mass and speed-of-light effects are included
- Charge separation is modeled
- Displacement current effects are resolved in the MFPM



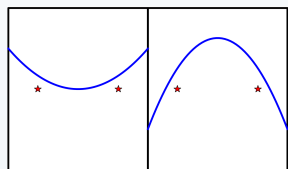
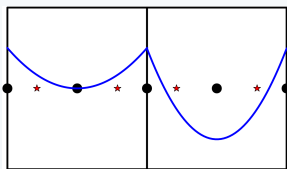
$$\frac{\partial \mathbf{Q}}{\partial t} + \frac{\partial \overleftarrow{\mathbf{F}}}{\partial \mathbf{x}} = \mathbf{S}$$

- The source Jacobian  $\frac{\partial \mathbf{S}}{\partial \mathbf{Q}}$  has imaginary eigenvalues
- The equation system has dispersive sources
- The dispersion is physical (may be difficult to distinguish from numerical dispersion)
- This dispersion is due to plasma waves that result from ion and electron plasma interactions with electromagnetic fields
- An ideal numerical method for the MFPM should:
  - be high-order accurate
  - capture shocks
  - couple the flux and the sources
  - not impose strict time-step





- Solution to the electron and EM fields is smooth and does not shock



- Continuous Galerkin
- Electron fluid and EM fields

$$\mathbf{Q} = \sum_i \mathbf{q}_i v_i$$

- Discontinuous Galerkin
- Multiple ion and neutral fluids

$$\mathbf{Q} = \sum_i \mathbf{c}_i v_i$$



- For this implementation the balance law form is cast as

$$\frac{\partial \mathbf{Q}}{\partial t} + \frac{\partial \overleftrightarrow{\mathbf{F}}}{\partial \mathbf{Q}} \cdot \frac{\partial \mathbf{Q}}{\partial \mathbf{x}} = \mathbf{S} + \kappa \nabla^2 \mathbf{Q}_d$$

- Lagrange polynomials are used for basis functions,  $v_r$

$$\int_{\Omega} v_r \frac{\partial \mathbf{Q}}{\partial t} dV = \mathcal{L}_r(\mathbf{Q}) = \int_{\Omega} v_r \mathbf{S} dV - \int_{\Omega} v_r \frac{\partial \overleftrightarrow{\mathbf{F}}}{\partial \mathbf{Q}} \cdot \frac{\partial \mathbf{Q}}{\partial \mathbf{x}} dV + \kappa \int_{\Omega} v_r \nabla^2 \mathbf{Q}_d dV$$

- $\theta$ -method time integration

$$\mathcal{R}(\mathbf{Q}^n) = \overleftrightarrow{\mathbf{M}} \frac{\mathbf{Q}^{n+1} - \mathbf{Q}^n}{dt} - \theta \mathcal{L}_r(\mathbf{Q}^{n+1}) - (1 - \theta) \mathcal{L}_r(\mathbf{Q}^n) = 0$$

- $\theta = 0.5$  is used for 2<sup>nd</sup> order accuracy

$$\overleftrightarrow{\mathbf{J}}(\mathbf{Q}^n) = \frac{\partial \mathcal{R}(\mathbf{Q}^n)}{\partial \mathbf{Q}^n}, \quad \overleftrightarrow{\mathbf{J}}(\mathbf{Q}^n) \Delta \mathbf{Q} = -\mathcal{R}(\mathbf{Q}^n), \quad \mathbf{Q}^{n+1} = \mathbf{Q}^n + \Delta \mathbf{Q}$$





$$\frac{\partial \mathbf{Q}}{\partial t} + \frac{\partial \overleftrightarrow{\mathbf{F}}}{\partial \mathbf{x}} = \mathbf{S}$$

- Legendre polynomials are used for basis functions,  $v_p$
- The hyperbolic equation is multiplied by the basis function,

$$\int_{\Omega} v_p \frac{\partial \mathbf{Q}}{\partial t} dV = \mathcal{L}_p(\mathbf{Q}) = \int_{\Omega} v_p \mathbf{S} dV - \oint_{\partial\Omega} v_p \overleftrightarrow{\mathbf{F}} \cdot d\mathbf{A} + \int_{\Omega} \overleftrightarrow{\mathbf{F}} \cdot \nabla v_p dV$$

- Explicit Runge-Kutta time integration
- $CFL = c\Delta t/\Delta x \leq 1/(2p - 1)$ ,  $p$  is the polynomial order

$$\mathbf{Q}^* = \mathbf{Q}^n + \Delta t \mathcal{L}_p(\mathbf{Q}^n),$$

$$\mathbf{Q}^{n+1} = \frac{1}{2} \mathbf{Q}^* + \frac{1}{2} \mathbf{Q}^n + \frac{1}{2} \Delta t \mathcal{L}_p(\mathbf{Q}^*).$$

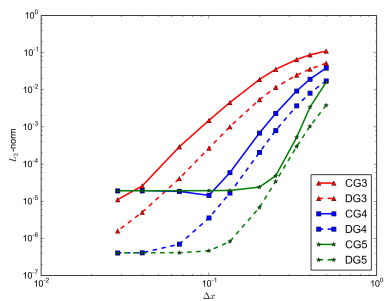




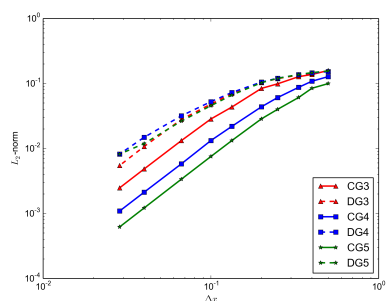
$$\frac{\partial Q}{\partial t} + \frac{\partial Q}{\partial x} = 0, \quad Q(x, 0) = e^{-10(x-8)^2},$$

$$\|\Delta Q\|_2 = \sqrt{\frac{1}{n} \sum_{i=1}^n (\hat{Q} - Q_i)^2}$$

## Spatial Convergence



## Temporal Convergence



- Simulations at fixed time-step



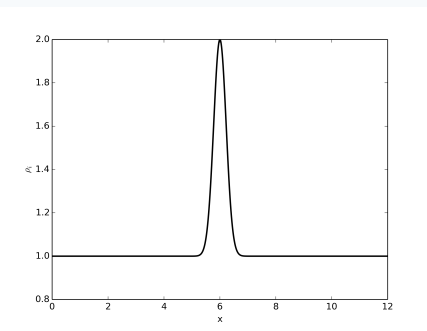
# 1D SOLITON PROBLEM



- 1D soliton is a two-fluid plasma problem
- The solution is smooth, therefore artificial dissipation can be small
- The simulation uses 512 second-order elements
- $B_z = 1.0, T_e = T_i = 0.01,$   
 $\mathbf{u}_i = \mathbf{u}_e = \mathbf{0}$
- $n_e = n_i = 1.0 + e^{-10(x-6)^2}$

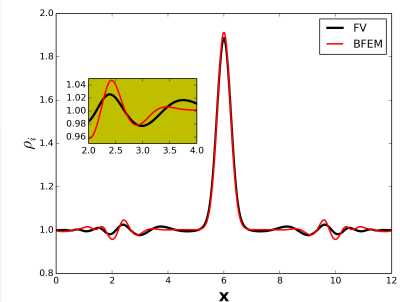
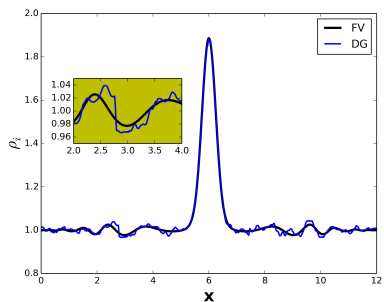


Baboolal, Math. and Comp. Sim. 55 (2001)





$$\frac{m_i}{m_e} = 1836, \frac{c}{c_{si}} = 1000\sqrt{2}, \text{ FV 5000 cells}$$



- DG Solution is very dispersive
- BFEM is less dissipative than the converged solution



Hakim et al, JCP 219 (2006)



# BFEM COMPUTATIONAL COST SAVINGS

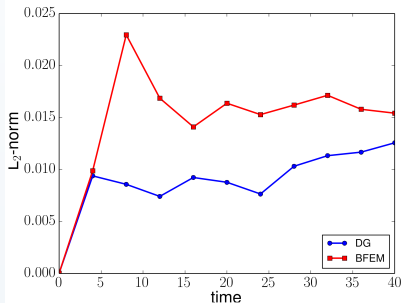


case	$m_i/m_e$	$c/c_{si}$	DG time(s)	BFEM time (s)	BFEM cost over DG
1	25	$10/\sqrt{2}$	0.32	37.7	+11681%
2	100	$10/\sqrt{2}$	1.28	37.7	+2845%
3	500	$10/\sqrt{2}$	6.82	37.7	+452.8%
4	1000	$10/\sqrt{2}$	12.4	38.2	+208.1%
5	1836	$10/\sqrt{2}$	23.5	40.4	+71.91%
6	3672	$10/\sqrt{2}$	47.2	39.2	-16.95%
7	3672	$100/\sqrt{2}$	520	265	-49.04%
8	3672	$1000/\sqrt{2}$	5274	2735	-48.14%

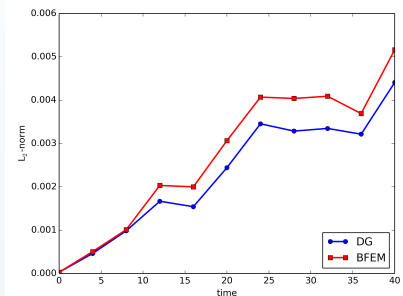
- Per time-step explicit DG is faster than BFEM, but it requires many more time-steps
- BFEM is more efficient only when time-step are considerably larger than explicit DG



# BFEM ACCURACY



$$m_i/m_e = 1836$$

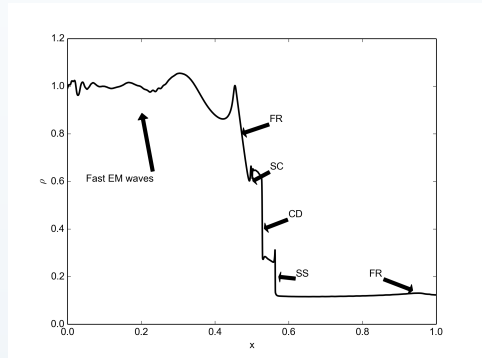


$$m_i/m_e = 1$$

- The BFEM seems to be less accurate than the DG implementation (~ 50%)
- When the mass ratio is one, the two methods have the same level of accuracy
- The discrepancy is due to the fact that the semi-implicit BFEM does not resolve the plasma frequency in this problem



- Fast rarefaction wave (FR), a slow compound wave (SC), a contact discontinuity (CD), a slow shock (SS), and another fast rarefaction wave (FR)
- The problem exhibits limits of MHD and multi-fluid behavior by changing the Larmor radius,  $r_L$ 
  - MHD:  $r_L \rightarrow 0$
  - Multi-fluid:  $r_L \sim L$



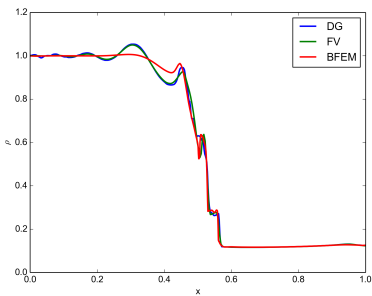
Brio and Wu, JCP 75 (1988)



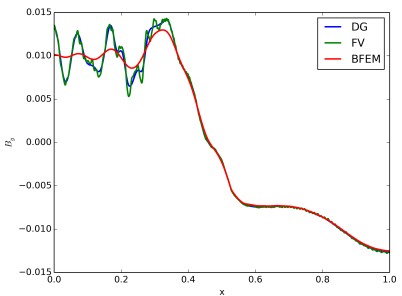
# SHOCK IN DENSITY BUT SMOOTH FIELDS.



- $t=0.05/\omega_{ci}$ ,  $c/c_{si}=110$ ,  $m_i/m_e=1836$



mass density



Magnetic field (y-comp.)

- The main features of the problem are captured by all three methods
- BFEM does not properly resolve the fast electromagnetic waves which require accurately resolving the electron dynamics

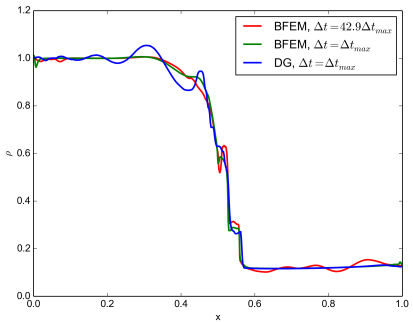


# MAXIMUM BFEM TIME-STEP



$$\Delta t_{max} = \min \left( \frac{\Delta x}{c_{se}}, \frac{\Delta x}{c_{si}}, \frac{\Delta x}{c}, \frac{0.1}{\omega_{ce}}, \frac{0.1}{\omega_{ci}}, \frac{0.1}{\omega_{pe}}, \frac{0.1}{\omega_{pi}} \right)$$

- $\Delta t_{max}$  corresponds to the maximum value allowed for explicit methods based on the CFL condition
- $\Delta t = 42.9\Delta t_{max}$  is the maximum time step allowed by the BFEM due to ion dynamics

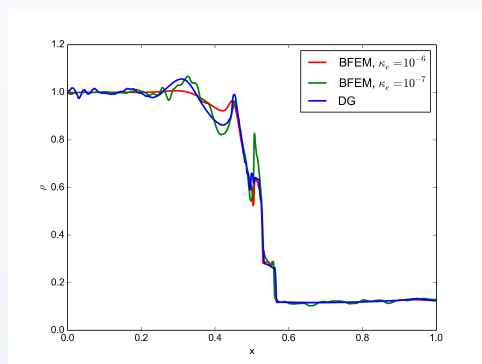




# EFFECTS OF ARTIFICIAL DISSIPATION



- Varying the artificial dissipation on the electron fluid,  $\kappa_e$
- Wave-like behavior of the problem is better resolved
- Amplitude of the compound wave increases
- Right fast rarefaction wave is not visible

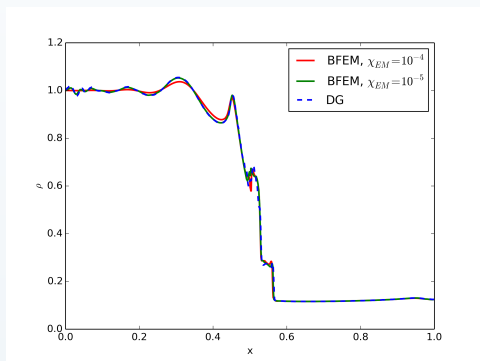




# EFFECTS OF ARTIFICIAL DISSIPATION



- Varying the artificial dissipation on the EM-field,  $\kappa_{EM}$
- There is better agreement with the DG solution
- This reinforces the point that the wave-like behavior arises from the interaction of the electron fluid with the electromagnetic fields





- The blended finite element method (BFEM) is presented
  - DG spatial discretization with explicit Runge-Kutta ( $i^+$ , n)
  - CG spatial discretization with implicit Crank-Nicolson ( $e^-$ , files)
  - DG captures shocks and discontinuities
  - CG is efficient and robust for smooth solutions
- Physics-based decomposition of the algorithm yields numerical solutions that resolve the desired timescales
- DG method takes less computational time to advance the solution by one time-step, however  $\Delta t$  is much smaller than that of the BFEM
- Computational cost savings using the BFEM will only occur for relatively large implicit time-steps compared to explicit time-steps



Sousa and Shumlak, JCP 326 (2016) 56-75

Thank you.



# EXTRAS





- Modeling each particle velocity and position is not practical.
- Instead an average is performed to give a statistical description.
- Calculate the number of particles per unit volume having approximately the velocity  $\mathbf{v}$  near the position  $\mathbf{x}$  and at time  $t$ , distribution function  $f(\mathbf{v}, \mathbf{x}, t)$

$$\rho_s = m_s \int f_s(\mathbf{v}) d\mathbf{v}$$

$$\rho_s \mathbf{u}_s = m_s \int \mathbf{v} f_s(\mathbf{v}) d\mathbf{v}$$

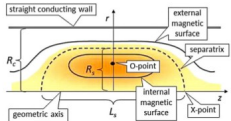
$$\mathbb{P}_s = \mathbf{P}_s = m_s \int \mathbf{w} \mathbf{w} f_s(\mathbf{v}) d\mathbf{v}, \quad p_s = \frac{1}{3} m_s \int w^2 f_s(\mathbf{v}) d\mathbf{v}$$

$$\mathbf{H}_s = m_s \int \mathbf{w} \mathbf{w} \mathbf{w} f_s(\mathbf{v}) d\mathbf{v}, \quad \mathbf{h}_s = \frac{1}{2} m_s \int w^2 \mathbf{w} f_s(\mathbf{v}) d\mathbf{v}$$

$$\mathbf{w} = \mathbf{v} - \mathbf{u}_s$$

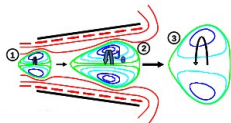
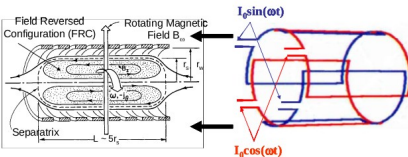


# FIELD REVERSED CONFIGURATION THRUSTER



- Compact toroid, no central column
- Simple geometry and B-field configuration
- High power density (high plasma beta)
- Highly movable

- A Rotating Magnetic Field (RMF) is used to form the FRC
- Strong magnetization of the electrons to the RMF produces a current
- To conserve the total flux the B-field at the center reverses



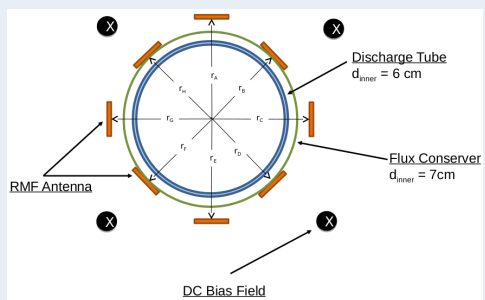
- 1 - Formation of high density FRC
- 2 - Acceleration of the FRC by Lorentz force
- 3 - FRC expands, converting thermal energy to directed energy

## Advantages:

- Electrodeless and the plasmoid propellant is magnetically isolated from the walls
- Propellant is completely uncoupled from the driving and confining fields
- High plasma temperatures and densities significantly reduce ionization losses



- The formation of FRC using a rotating magnetic field (RMF)
- $\omega_{ci} < \omega < \omega_{ce}$
- $\nu_{ei} \ll \omega_{ce}$



- Flux Conserver BC

$$B_z(a, t) = \frac{b^2 B_a(0)}{b^2 - a^2} - \frac{1}{\pi(b^2 - a^2)} \int_0^a r dr \int_0^{2\pi} d\theta B_z(r, \theta, t)$$

- RMF BC

$$\begin{aligned} I_{RMF} &= I_t \cos(\omega t + \phi) \\ I_t &= I_o (1 - e^{-t/\tau}) \end{aligned}$$

- $\phi_{A,B} = 0, \phi_{E,F} = \pi$
- $\phi_{C,D} = \pi/2, \phi_{G,H} = -\pi/2$
- Bias Field is constant at t=0s

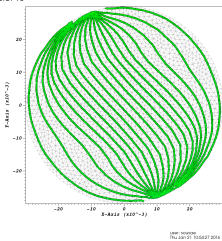


# RMF ANTENNA MODELING.

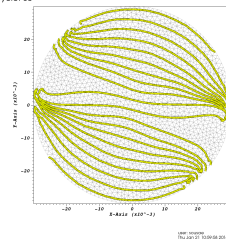


- Initialization:  $B_\omega=90G$ ,  $B_z=50G$ ,  $\omega=5MHz$
- Solve Maxwell's eqns. with divergence constraints

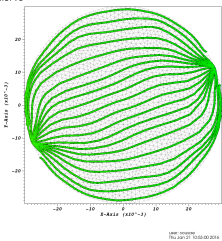
DB: cylindrical\_frcX\_Maxwell\_015.vtu  
Cycle: 15



DB: cylindrical\_frcX\_Maxwell\_050.vtu  
Cycle: 50



DB: cylindrical\_frcX\_Maxwell\_090.vtu  
Cycle: 90

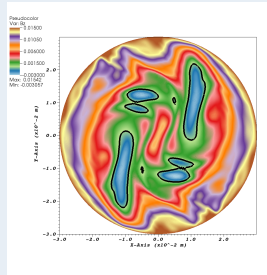




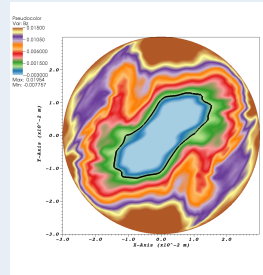
## FRC FORMATION SIMULATIONS.



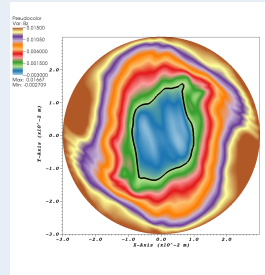
- Initialization:  $T_i = T_e = 30 \text{ eV}$ ,  $n_i = n_e = 10^{19} \text{ m}^{-3}$ ,  $m_i/m_e = 1836$
- Solve Multi-Fluid eqns.
- $B_z$  is plotted



$$t = 250\text{ns}$$



$$t = 500\text{ns}$$

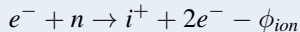


$$t = 1500ns$$



## Neutral-Plasma Model

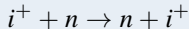
- Interaction of multi-fluid plasma with gas dynamics neutral fluid
  - electron-impact ionization



- radiative recombination



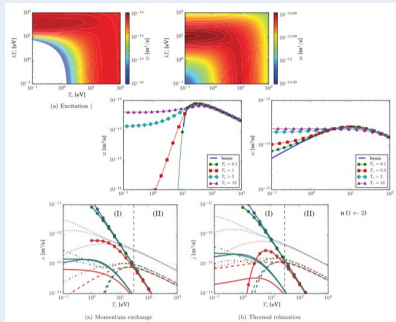
- resonant charge exchange



Meier and Shumlak, PoP 19 072508 (2012)

## Collisional-Radiative Model

- Excitation/De-excitation rates



Le and Cambier, PoP 22 093512 (2015)